J. Chem. Soc. Nigeria, Vol. 47, No. 4, pp 739 – 758 [2022]

THEORETICAL INVESTIGATIONS OF THE OPTOELECTRONIC PROPERTIES OF SOME 2, 4, 5-TRIPHENYL IMIDAZOLE BASED DYES FOR PROBABLE USE AS DYE-SENSITIZED SOLAR CELLS

S. A. Ahmed[*1], O. O. James[1], R. S. Ahmed[1] and S. Salau[1]

[1]Department of Chemistry and Industrial Chemistry, Kwara State University, Malete, Ilorin, Nigeria

(Corresponding author: akinyeye.ahmed@kwasu.edu.ng)

ABSTRACT

The fast growing global demand for energy and the diminishing negative environmental effects associated with the burning of fossil fuels have forced the rapid development of renewable energy technology. In comparison to silicon-based semiconductor solar cells, dye-sensitized solar cells (DSSCs) offer a fascinatingly low cost of photovoltaic energy conversion, which has attracted a lot of attention. This work focuses on the investigation of photovoltaic, optical, and electronic absorption properties of some 2, 4, 5-triphenyl imidazole based dyes using Time Dependent-Density Functional Theory (TD-DFT) via a Donor-π-Acceptor (D-π-A) framework. Results obtained show that most compounds with a cyanoacetic acceptor unit are much more favoured for Dye-Sensitive Solar Cells (DSSCs) applications than those without. Also, the electronic injection free energy (ΔG_{inject}) was observed to have the highest value in TPI6 (-0.86 eV) due to the presence of a cyanoacetic acceptor. Furthermore, Absorbance data revealed how dyes containing cyanoacetic acceptor units tend to absorb both visible and UV light while dyes lacking the strong cyanoacetic acceptor groups absorbed only at the electromagnetic spectrum.

Keywords: DSSC, Imidazole, Optoelectronic, TD-DFT, Photovoltaic, Donor-π-Acceptor

INTRODUCTION

The rapid development of renewable energy technologies has been necessitated by the steadily increasing global demand for energy, as well as the depletion of harmful environmental effects associated with the combustion of fossil fuels [1], [2]. Due to the fascinating low cost of photovoltaic energy conversion compared to silicon-based semiconductor solar cells, dye-sensitized solar cells (DSSCs) have gotten [3], [4] a lot of attention. A wide band gap semiconductor, the sensitizer (dye molecules), a transparent conductive oxide layer (TCO), and a redox electrolyte (typically iodide/triiodide) are the main components of DSSCs [2]. The dye absorbs solar radiation in the visible spectrum and excites an electron into the semiconductor's conductive band; the redox electrolyte then regenerates an electron to the dye [5].

ISSN 0795 - 22066

Metal-free natural dyes have recently garnered considerable attention, whilst organometallic dye complexes haven't. This is because of their low toxicity, high molar extinction coefficient, ease of access, light weight, and cost effectiveness [5]. As a result, scientists are working to develop a metal-free organic dye for use in dye-sensitized solar cells [6]. Unfortunately, they have narrow optical absorption spectra, which makes it difficult to achieve the maximum short-circuit current density (J_{sc}), resulting in a lower power conversion efficiency (~9.5%) [7].

The most extensively studied organic dyes usually adopt the donor-π-spacer-acceptor (D-π-A) structural motif, which exhibit several advantages: high molar extinction coefficients, low cost of production, and an extraordinary diversity [8]. In this structure, the intramolecular charge transfer (ICT) from D to A at the photo excitation will inject the photoelectron into the conduction band of the semi-conductor through the electron accepting group at the anchoring unit. By changing the electron donor, acceptor, and/or π-spacer group, the HOMO and LUMO energy levels are affected [9].

Imidazole, being one of the nitrogen-containing heterocyclic compounds has a lot of application and are currently a subject of intense research [10]. Amongst the numerous documented applications of Imidazoles and its moieties are its reported biological activities [11], its use as starting material or precursor for other synthetics compounds/derivatives [12], its pharmacological properties [13] and its reported use as dye sensitizer [14] among others.

The imidazole pharmacophore's effectiveness and broad applicability can be due to its hydrogen bond Donor-Acceptor ability and strong affinity for metals (such as Zn, Fe, and Mg), which are found in numerous protein active sites [15]. Naturally occurring substituted imidazoles, as well as synthetic derivatives thereof, exhibit wide ranges of physical and biological activities, making them attractive compounds for both organic and physical chemists.

The ability to design molecular structures at the molecular level, and that can favorably be studied alongside experimental feedback of already-existing dye sensitizers, can be provided by density functional theory (DFT) [15], [16]. Hence, this study focuses on the TD-DFT investigation of photovoltaic, optical and absorption properties of some potential DSSC through a D-π-A of 2, 4, 5-triphenyl imidazole framework.

MATERIALS AND METHODS

All computational calculations were done using the Gaussian® 09W Revision package

ISSN 0795 - 22066

software [17], visualizations software includes Avogadro® version 1.2.0 [18] while graphical representations were done using, Multiwfn® package version 3.8 [19] and Origin Lab® 2021 edition [20]. Lastly, all compounds were modelled using the ChemDraw® Ultra drawing tool [21]. TPI1 (2, 4, 5-triphenyl imidazole) and its nine derivatives were studied. The derivatives were modelled by substituting the donor group in para- position to the phenyl rings 2 and 3 of the imidazole structure at the C4 and C5 positions, respectively.

The derivatives investigated includes, 2,4,5-triphenyl-1H-imidazole (TPI1), 4,5-bis(4-chlorophenyl)-2-phenyl-1H-imidazole (TPI2), 4,5-bis(4-methoxyphenyl)-2-phenyl-1H-imidazole (TPI3), (E)-3-cyano-2-(4-(4,5-diphenyl-1H-imidazol-2-yl)phenyl)phenyl)acrylic acid (TPI4), (Z)-2-(4-(4,5-bis(4-methoxyphenyl)-1H-imidazol-2-yl)phenyl)-3-cyanoacrylic acid (TPI5), (Z)-2-(4-(4,5-bis(4-chlorophenyl)-1H-imidazol-2-yl)phenyl)-3-cyanoacrylic acid (TPI6), (E)-2-(4-(4,5-bis(4-methoxyphenyl)-1-methyl-1H-imidazol-2-yl)phenyl)-3-cyanoacrylic acid (TPI7), (E)-3-cyano-2-(4-(1,4,5-triphenyl-1H-imidazol-2-yl)phenyl)acrylic acid (TPI8), (Z)-3-cyano-2-(4-(1,4,5-tris(4-methoxyphenyl)-1H-imidazol-2-yl)phenyl)acrylic acid (TPI9), and (E)-3-cyano-2-(4-(1,4,5-tris(4-chlorophenyl)-1H-imidazol-2-yl)phenyl)acrylic acid (TPI10).

Method validation procedure was done via DFT/B3LYP (Becke three-parameter Lee-Yang-Parr) [22] technique (with split valence orbitals) such as 3-21G(d,p), 6-31+G(d,p), 6-31++G(d,p) and CAM-B3LYP/6-31G(d,p) (Coulomb Attenuated-B3LYP) in comparison with experimental data in solvent (methanol) phase [23] to study the theoretical basis set that is suitable enough for the study. For effective comparative sake, each basis-set was used both to optimize and calculate for excitation energies of 2, 4,5-triphenyl imidazole in solvent (methanol).

After optimization in solvent phase, the excited state energies, electron absorption spectra, and oscillator strengths (*f*) were investigated using the TD-DFT/B3LYP method

ISSN 0795 - 22066

with the 6-31+G (d, p) basis set. The polarizable continuum model (PCM) was used for all computations in the solvent phase.

RESULTS AND DISCUSSION

Method validation

Figure 1 shows the plots from both experimental data and theoretical data. Excitation values, interpreted into table 1 reveal that the DFT method at 6-31+G (d, p) is most appropriate. Hence, DFT-B3LYP/6-31+G(d,p) level of theory was adopted in this study.

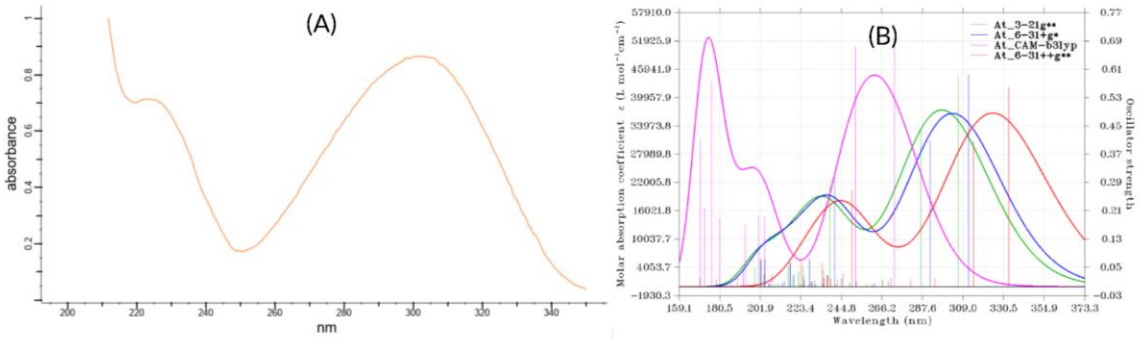

Figure 1: Comparative excitation energy plots of the (A) Experimental data (in methanol) [5] and (B) Theoretical modeling data of 2,4,5- tri-phenyl imidazole (in methanol) at different level of theory.

Table 1: Summarizing the DFT excitation-energy modeling of 2,4,5-tri-phenyl imidazole at different level of theory in solvent phase.

Excitation	Experimental value (nm)	3-21G(d,p) (nm)	6-31+G(d,p) (nm)	CAM-B3LYP (nm)	6-31++G(d,p) (nm)
S_0-S_1	303	308.5	309.9	268.2	331.1
S_0-S_2	224.7	232.1	234.4	249.1	309

ISSN 0795 - 22066

Geometry structural optimization

The optimized geometry structure of all dye compounds studied, at B3LYP/6-31+G(d,p) level of theory are illustrated in Figure 2. As opposed to Juma *et al.*, [2], all the compounds showed a non-coplanar geometry which indicates that the compounds are capable of improving electron transfer from donor (D) to acceptor (A) through the π–spacers. As shown in table 2, the minimization energy of the dye compounds (E_{min}), at B3LYP/6-31+G(d,p) level of theory is found to be -24880.42, -49754.38, -31078.93, -39981.18, -40772.23, -59466.37, -41836, -40826.21, -50124.14, -78165.17 eV for TPI1-TPI10 respectively.

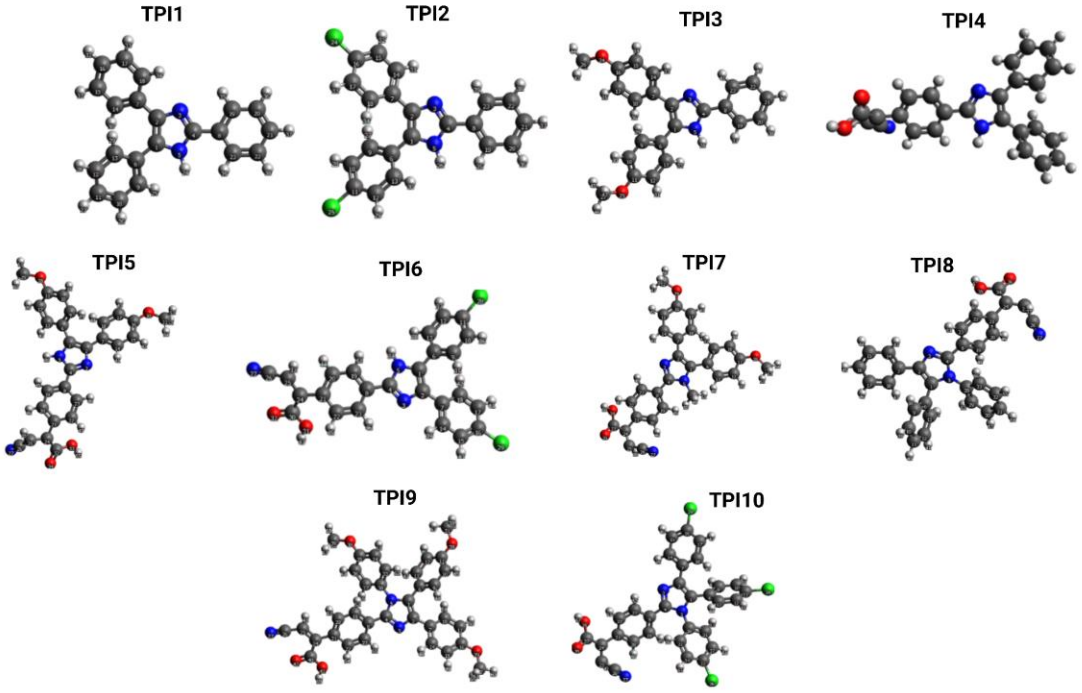

Figure 2: Optimized structure of compounds in solvent phase at B3LYP/6-31+G(d,p) level.

Frontier molecular orbital theory

An important characteristic an organic dye must possess to qualify for DSSC application is the intramolecular charge transfer (ICT) from the donor to the anchoring group through the π-spacer. This attribute is dependent on the energy gap and the photocurrent of the molecule [15], [24].

ISSN 0795 - 22066

Frontier molecular orbital theory comprises of Highest occupied molecular orbital (HOMO) and Lowest unoccupied molecular orbital (LUMO). HOMO orbital depicts bonding character while LUMO orbital, anti-bonding character. Table 3 reveals that all HOMO exhibits aromatic natures due to electron de-localization [3] while LUMO are majorly concentrated at the acceptor units.

It is said that compound with high electric dipole moment are more sensitive to external electric field [24]. Results show that the cyanoacetic acceptor units (TPI4-TPI10) contributes significantly to the reactivity of the anchoring group than those without the acceptor groups (TPI1-TPI3). According to Table 2, the rate of sensitivity due to electric dipole moment follows the order of TPI8>TPI7>TPI5>TPI4>TPI3>TPI10>TPI1 >TPI6>TPI9. The difference in the energy of HOMO and LUMO is given by the Energy gap (E_g). The energy gap can be explained further as the ease of electron excitation from ground state (HOMO) to excited state (LUMO). Results in Table 2 points to the fact that compounds with cyano-acetic acceptor units (TPI4-TPI10) exhibits lower energy gaps compared to those without. This means that excitation is most favored in compounds with cyano-acetic acceptor units than those without.

Table 2: Energy values of HOMO (E_{HOMO}), LUMO (E_{LUMO}) and gap (E_{gap}) of the solvated studied compounds calculated using B3LYP/6-31+G (d,p) level

Dyes	E_{HOMO} (eV)	E_{LUMO} (eV)	E_{Min} (eV)	E_g (eV)	μ (debye)
TPI1	-5.21	-1.06	-24880.42	4.15	3.54
TPI2	-5.51	-1.43	-49754.38	4.07	6.25
TP3	-4.88	-0.87	-31078.93	4.01	4.79
TPI4	-5.32	-2.87	-39981.18	2.45	5.35
TPI5	-5.10	-2.86	-40772.23	2.24	6.47
TPI6	-5.73	-2.86	-59466.37	2.87	3.22
TPI7	-5.23	-4.16	-41836.00	1.06	6.96
TPI8	-5.59	-4.30	-40826.21	1.28	7.36
TPI9	-5.07	-2.65	-50124.14	2.42	2.15
TPI10	-5.66	-4.28	-78165.17	1.37	3.50

ISSN 0795 - 22066

Table 3: HOMO-LUMO diagram of the first electron excitation of TPI1-TPI10 at 6-31+G (d,p) level.

	Structure	HOMO	LUMO
TP1	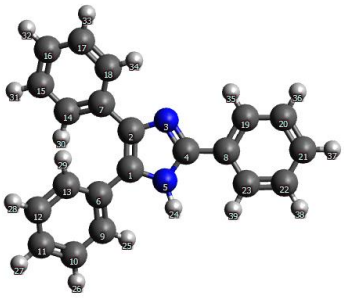	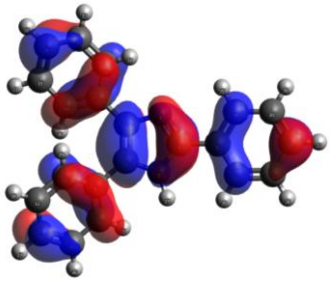	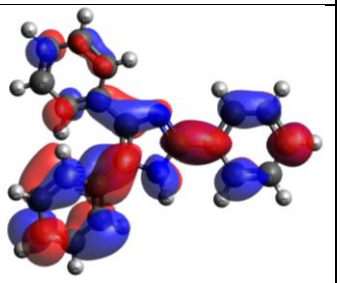
TP2	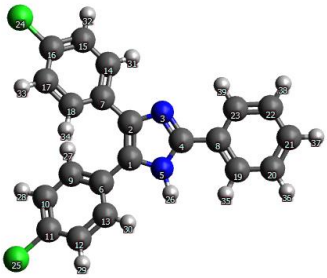	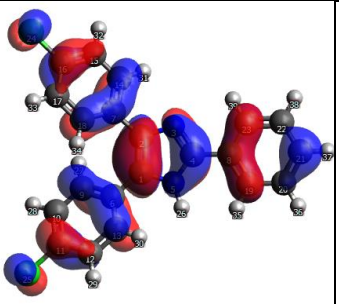	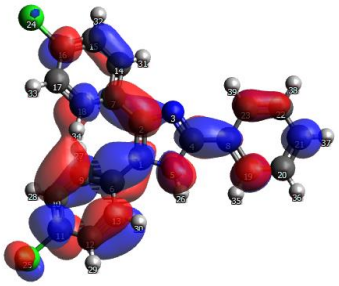
TP3	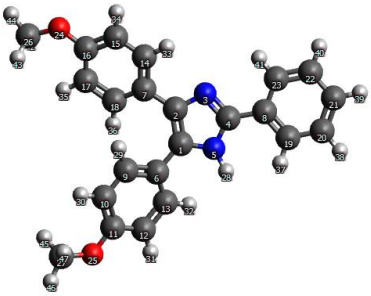	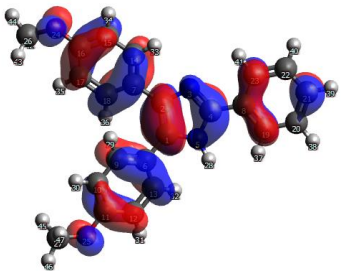	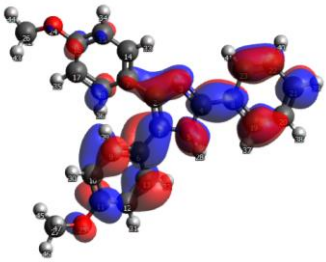
TP4	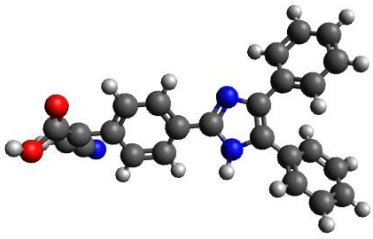	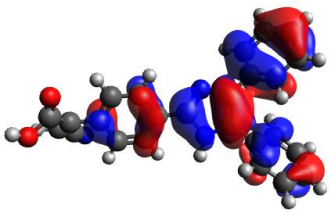	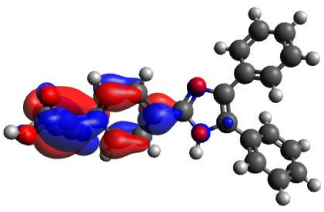

ISSN 0795 - 22066

TP5	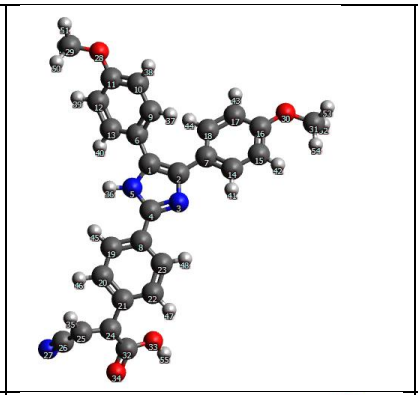	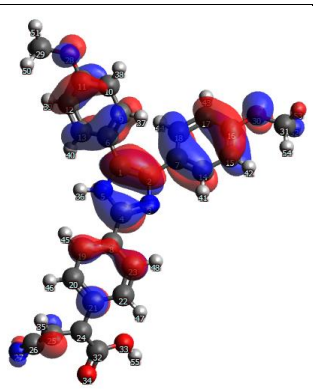	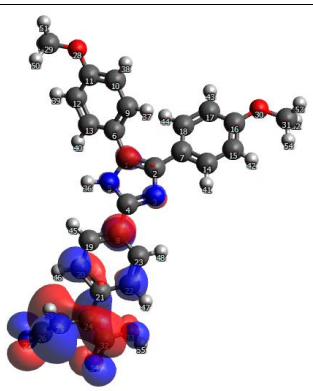
TP6	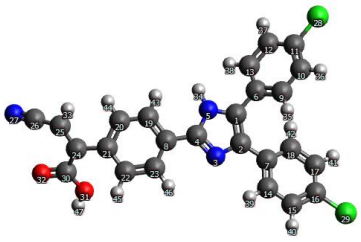	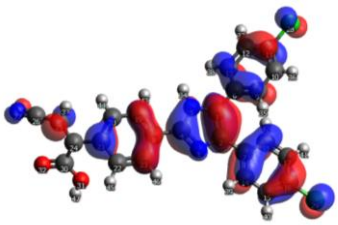	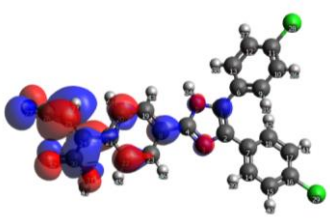
TP7	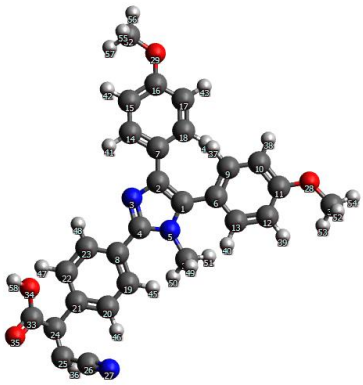	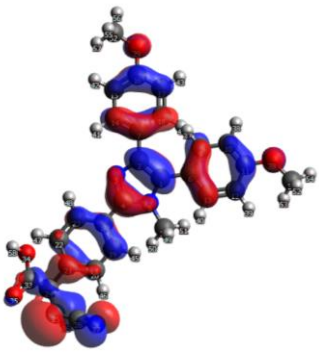	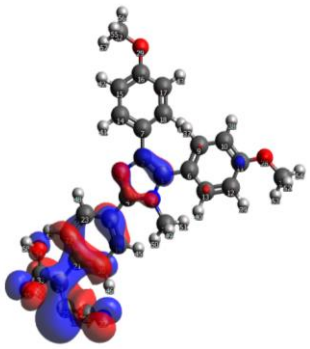
TP8	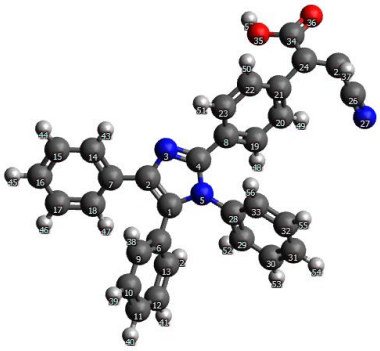	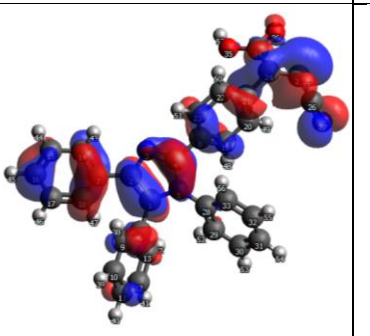	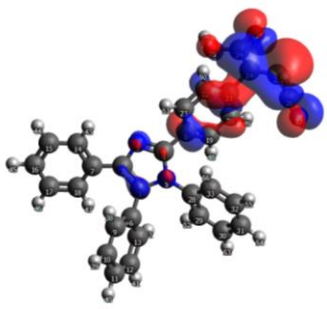
TP9	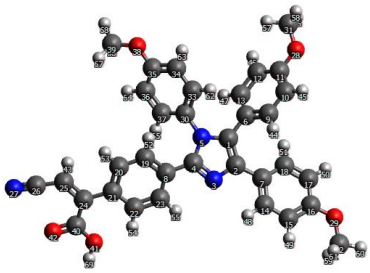	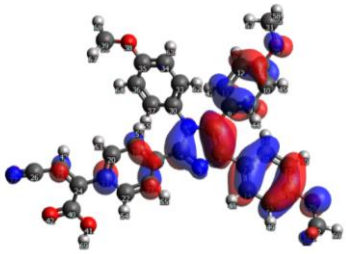	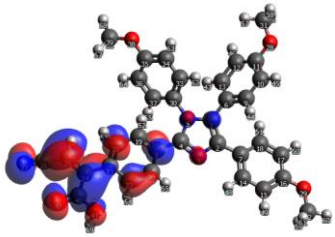

ISSN 0795 - 22066

TP10	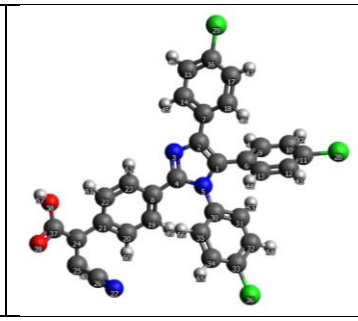	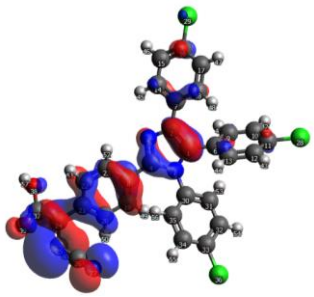	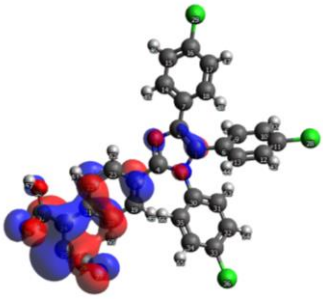

The HOMO-LUMO energy plots is shown in Figure 3 with respect to the redox potential and oxidation potential of Iodide/triiodide (-4.8 eV) and titanium (IV) oxide (-4.0 eV) respectively. Results show that despite TPI7, TPI8 and TPI10 showing lower E_g values, they are unsuitable for DSSC purposes due to their lower HOMO values. However, of all the cyano-acetic acceptor units, TPI4, TPI5, TPI6, and TPI9 are found to be suitable for DSSC applications.

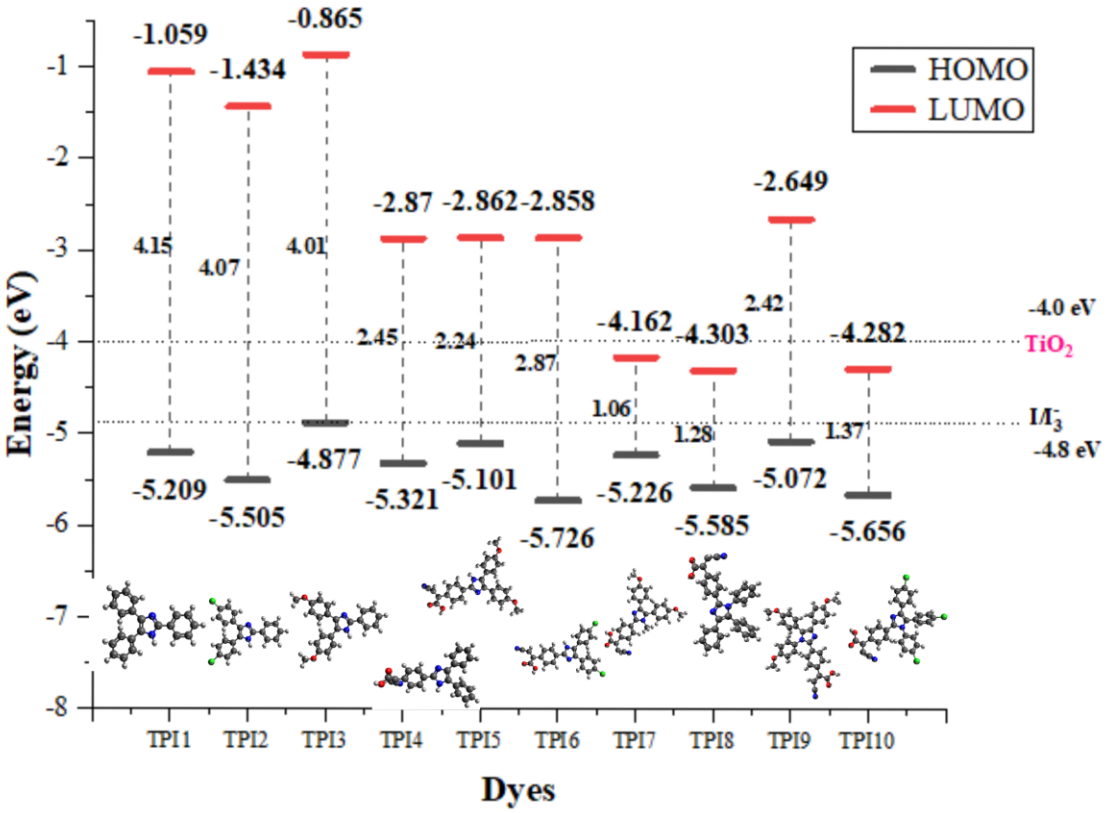

Figure 3: Plot of HOMO-LUMO values and energy band gaps for solvated TPI1-TPI10 at 6-31+G(d,p) level.

ISSN 0795 - 22066

Theoretical background of some parameters

1. Photovoltaic properties

The power conversion efficiency is the percentage of solar energy that is turned into useable electricity by a solar cell device. The following formula was used to compute the power conversion efficiency (η).

$$\eta = FF\frac{V_{oc}J_{sc}}{P_{inc}} \qquad 1$$

where P_{inc} is the incident power density, J_{sc} is the short-circuit current, V_{oc} is the open-circuit voltage, and *FF* denotes the fill factor. In other to analyze the relationship between V_{oc} and E_{LUMO} of the dyes based on electron injection (in DSSCs) from LUMO to the conduction band of the TiO_2 semiconductor, $E_{RDP}^{TiO_2}$. The energy relationship can be expressed as:

$$V_{oc} = E_{LUMO} - E_{RDP}^{TiO_2} \qquad 2$$

The following equation determines the short-circuit current density (J_{sc}) in DSSCs [25],

$$J_{sc} = \int LHE\,(\lambda)\Phi_{inject}\eta_{collect}d\lambda, \qquad 3$$

where LHE (λ) is the light-harvesting efficiency at a given wavelength, Φ_{inject} is the electron injection efficiency, and $\eta_{collect}$ denotes the charge collection efficiency. In the system where there are only differences in dye, $\eta_{collect}$ can be assumed to be constant. The LHE can be calculated through the following equation [9]:

$$LHE = 1 - 10^{-f} \qquad 4$$

where f is the oscillator strength of adsorbed dye molecules. Φ_{inject} is related to the driving force (ΔG_{inject}) of electrons injecting from the excited states of dye molecules to the semiconductor (conduction band). It can be estimated as follows [3]:

$$\Delta G_{inject} = E_{OX}^{dye*} - E_{CB}^{TiO_2} = E_{OX}^{dye} + E_{0-0}^{dye} - E_{CB}^{TiO_2} \qquad 5$$

From the equations (1), (2), (3), (4), and (5), we could predict theoretically the efficiency of the novel triphenyl derivatives without intensive calculations. In the above equations,E_{OX}^{dye*} is the oxidation potential of the excited dye, E_{OX}^{dye} is the oxidation potential of

ISSN 0795 - 22066

the ground state of the dye, E_{0-0}^{dye*} is the vertical transition energy, and $E_{CB}^{TiO_2}$ is the conduction band edge of the TiO_2 semiconductor. Hence, J_{sc} can be well estimated through LHE and ΔG_{inject}.

Given the above equations 1-5, the light harvesting efficiency of the compounds TPI1-TPI10 can be predicted theoretically.

E_{OX}^{dye*} can be evaluated from equation 6 which can be extracted from the oxidation potential of ground state, E_{OX}^{dye} and the maximum absorbance (λ_{max}) in electron volts of the dye compound.

$$E_{OX}^{dye*} = E_{OX}^{dye} - \lambda_{max} \quad (6)$$

2. *Electron injection*

The broad classical Marcus theory may be used to get the description of electron transfer from a dye to a semiconductor and the rate of charge transfer [26]–[28].

In equation (8), k_{inject} is the rate constant (in s^{-1}) of the electron injection from dye to TiO_2, k_B is the Boltzmann thermal energy, h is the Planck constant, G_{inject} is the free energy of injection, and V_{RP} is the coupling constant between the reagent and the product potential curves. According to Equation (7), a greater V_{RP} leads to a higher rate constant, resulting in a superior sensitizer. V_{RP} for a photo induced charge transfer may be evaluated using the extended Mulliken-Hush (GMH) formalism [26].

The driving force of electron injection, E_{RP} can be expressed within Koopman's approximation as in equation (8) [16]. The coupling constant between reagent and product potential curves, V_{RP} value can be gotten from equation (9).

$$k_{inject} = V_{RP}\left(2/h\,(\pi/\lambda\, k_B T)\right) 1/2\ \ exp\left[-\left(\Delta G_{inject} + \lambda\right) 2/4\,\lambda K_B T\right] \quad (7)$$

$$\Delta E_{RP} = \left[E_{LUMO}^{dye} + 2E_{HOMO}^{dye}\right] - \left[E_{LUMO}^{dye} + E_{HOMO}^{dye} + E_{RDP}^{TiO_2}\right] \quad (8)$$

ISSN 0795 - 22066

where $E_{RDP}^{TiO_2}$, is the redox potential of TiO_2 which equals −4.0 eV [12] which is an experimental value corresponding to conditions where the semiconductor is in contact with aqueous redox electrolytes of fixed pH 7.0.

$$V_{RP} = \frac{\Delta E_{RP}}{2} \qquad 9$$

Table 4: Calculated theoretical values of photovoltaic parameters and open circuit voltage (V_{oc}) of the solvated studied compounds using B3LYP/6-31+G (d,p) level

Dyes	E_{OX}^{dye} **(eV)**	E_{OX}^{dye*} **(eV)**	**ΔG$_{inject}$ (eV)**	**LHE**	**V$_{OC}$ (eV)**	V_{RP} **(eV)**
TPI1	5.21	1.42	-2.58	0.65	2.94	0.61
TPI2	5.51	1.82	-2.19	0.64	2.57	0.75
TPI3	4.88	1.23	-2.77	0.65	3.14	0.44
TPI4	5.32	0.70	-3.30	0.63	1.13	0.66
TPI5	5.10	0.66	-3.34	0.52	1.14	0.55
TPI6	5.73	3.14	-0.86	0.57	1.14	0.86
TPI7	5.23	1.44	-2.56	0.66	0.16	0.61
TPI8	5.59	4.38	0.38	0.36	0.3	0.79
TPI9	5.07	0.76	-3.24	0.41	1.35	0.54
TPI10	5.66	2.3	-1.70	0.54	0.28	0.83

From the studied dye derivatives, the values of V_{oc} were calculated according to the equation (2) and values obtained range from 0.3 eV to 3.14 eV as shown in Table 4; this is in agreement with submission of Juma *et al.* [2] which confirms that the values obtained are sufficient for a possible efficient electron injection. Table 4 presents the photovoltaic properties in form of maximum absorbance (λ_{max}), driving force for electron injection (ΔG_{inject}), ground state oxidation potential (excited state oxidation potential) and Light

ISSN 0795 - 22066

Harvesting Efficiency (LHE). The short-circuit current J_{sc} depends on two main influencing factors: light- harvesting efficiency (LHE) and the electronic injection free energy (ΔG_{inject}) (in equation (3)). Likewise, the V_{oc} and the V_{RP} values depends on ΔG_{inject} .The LHE is a critical factor for organic dyes because it gives insight into the role of dyes in the DSSC in terms of absorbing photons and injecting photo-excited electrons into the semiconductor's (TiO_2).conduction band.

In Table 4, the calculated LHE values for all dye compounds range between 0.36 and 0.66.which indicate good harvesting power for all dye compounds.

Table 4 also reveals that ΔG_{inject} are negative for all dye compounds except for TPI8. This can be due to the lack of donor groups at the first and second phenyl ring, attached to the imidazole framework. Also, ΔG_{inject} values obtained are negative for all dye compounds except for TPI8. The reason can be ascribed to the fact that TPI8 lack the donor groups at the first and second phenyl ring, attached to the imidazole framework. Since the ΔG_{inject} values are negative, it implies that the electron injection process from the LUMO of the dye to the TiO_2 surface is favourable and spontaneous for all dye compounds [4]. Following this, out of the ten (10) dye compounds studied, TPI6 (-0.86 eV) have a larger ΔG_{inject}. Consequently, based on the ΔG_{inject} values in table 4, it is evident that of all the ten (10) dye compounds studied, TPI6 (-0.86 eV) has the highest ΔGinject. With reference to equations 3. 5 and 6 which mathematically connect the ΔG_{inject} and LHE to J_{sc}, it can be inferred that TPI6 will have a higher J_{sc}, than the remaining dye compounds in this study, and also, than the best dye compound reported in (-0.94 eV).

In summary, the results obtained show that TPI6 has the largest electron injection value among the rest of the studied dye compounds, while, the lowest electron injection value observed in TPI8 was due to the absence of auxochromic donor units at the para- position of the C4, C5 and N1 phenyl rings.

3. Absorption properties

Table 5 shows the computed excitation energies, oscillator strength and excited compositional states of the dye compounds. It is observed that the vertical energy changes with respect to the kind of donor group attached at the para- position of phenyl rings at C4, C5 and N1 positions. From the results in Table 5, the correlation between the ease of electron delocalization within the dye compounds and

ISSN 0795 - 22066

the maximum vertical transition of each dye compound was also revealed

Electronic absorption spectra of the studied dye compounds in figure 4 and 5 show that TPI4 – TPI10 have vertical energy absorbance in both UV and Visible regions whereas TPI1 – TPI3 absorb only in the UV region and this observation can be attributed to the presence of the cyanoacetic acceptors in the former compounds. This observation is in complete agreement with the submission of Malcioğlu et al. [29] that a potential dye compound for DSSC should absorb both in the UV and visible regions for easy electron injection and regeneration DSSC process.

Table 5: Absorption spectra data of the solvated TPI1-TPI10 compounds calculated with TD-DFT/6-31+G (d, p) level.

Dyes	Excited state	Main composition	λ_{max} (nm)	λ (eV)	*f*
TPI1	$S_0 \rightarrow S_1$	HOMO→LUMO	326.89	3.7928	0.452
	$S_0 \rightarrow S_2$	HOMO→LUMO	299.64	4.1377	0.295
	$S_0 \rightarrow S_6$	HOMO→LUMO	253.24	4.8960	0.253
TPI2	$S_0 \rightarrow S_1$	HOMO→LUMO	336.01	3.6899	0.442
	$S_0 \rightarrow S_3$	HOMO→LUMO	294.54	4.2094	0.253
	$S_0 \rightarrow S_6$	HOMO→LUMO	262.84	4.7171	0.283
TPI3	$S_0 \rightarrow S_1$	HOMO→LUMO	339.39	3.6531	0.460
	$S_0 \rightarrow S_3$	HOMO→LUMO	300.24	4.1295	0.253
	$S_0 \rightarrow S_5$	HOMO→LUMO	273.51	4.5330	0.314
TPI4	$S_0 \rightarrow S_1$	HOMO→LUMO	467.85	2.6501	0.246
	$S_0 \rightarrow S_{13}$	HOMO→LUMO	268.40	4.6193	0.428
	$S_0 \rightarrow S_{17}$	HOMO→LUMO	256.76	4.8288	0.421
TPI5	$S_0 \rightarrow S_1$	HOMO→LUMO	617.63	2.0074	0.269
	$S_0 \rightarrow S_4$	HOMO→LUMO	346.34	3.5798	0.291
	$S_0 \rightarrow S_{14}$	HOMO→LUMO	279.05	4.4430	0.322
TPI6	$S_0 \rightarrow S_1$	HOMO→LUMO	479.42	2.5861	0.363
	$S_0 \rightarrow S_3$	HOMO→LUMO	333.62	3.7164	0.277
	$S_0 \rightarrow S_5$	HOMO→LUMO	306.71	4.0423	0.262

ISSN 0795 - 22066

TPI7	$S_0 \rightarrow S_2$	HOMO→LUMO	945.92	1.3107	0.244
	$S_0 \rightarrow S_{15}$	HOMO→LUMO	327.46	3.7862	0.469
	$S_0 \rightarrow S_{17}$	HOMO→LUMO	299.16	4.1444	0.003
TPI8	$S_0 \rightarrow S_2$	HOMO→LUMO	1026.99	1.2073	0.191
	$S_0 \rightarrow S_{15}$	HOMO→LUMO	323.51	3.8325	0.158
	$S_0 \rightarrow S_{17}$	HOMO→LUMO	290.79	4.2636	0.001
TPI9	$S_0 \rightarrow S_1$	HOMO→LUMO	525.24	2.1553	0.210
	$S_0 \rightarrow S_5$	HOMO→LUMO	287.64	4.3104	0.232
	$S_0 \rightarrow S_{22}$	HOMO→LUMO	256.35	4.8366	0.219

ISSN 0795 - 22066

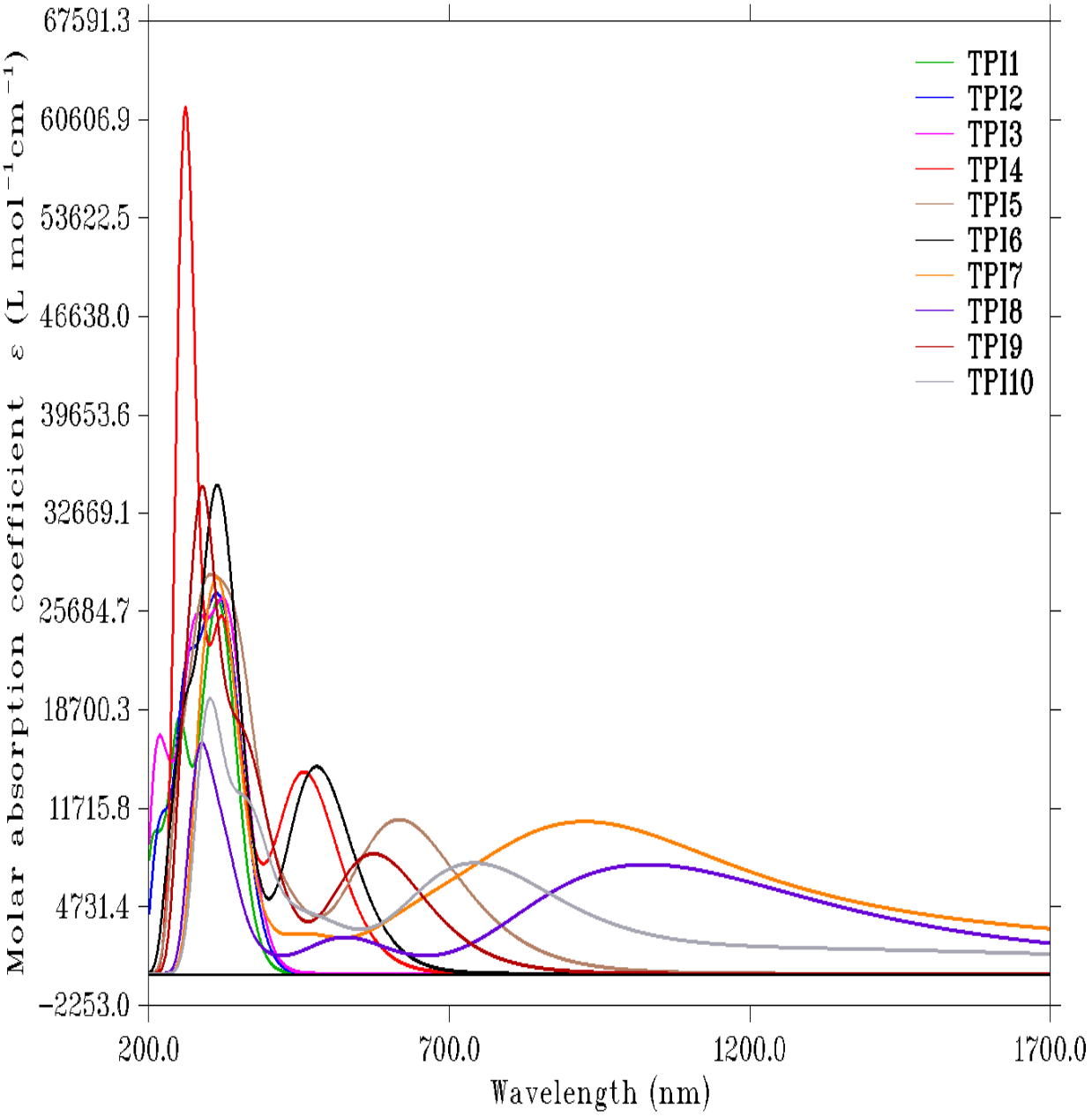

Figure 4: UV-Visible absorption spectra of solvated TPI1-TPI10 at 6-31+G(d,p) level.

ISSN 0795 - 22066

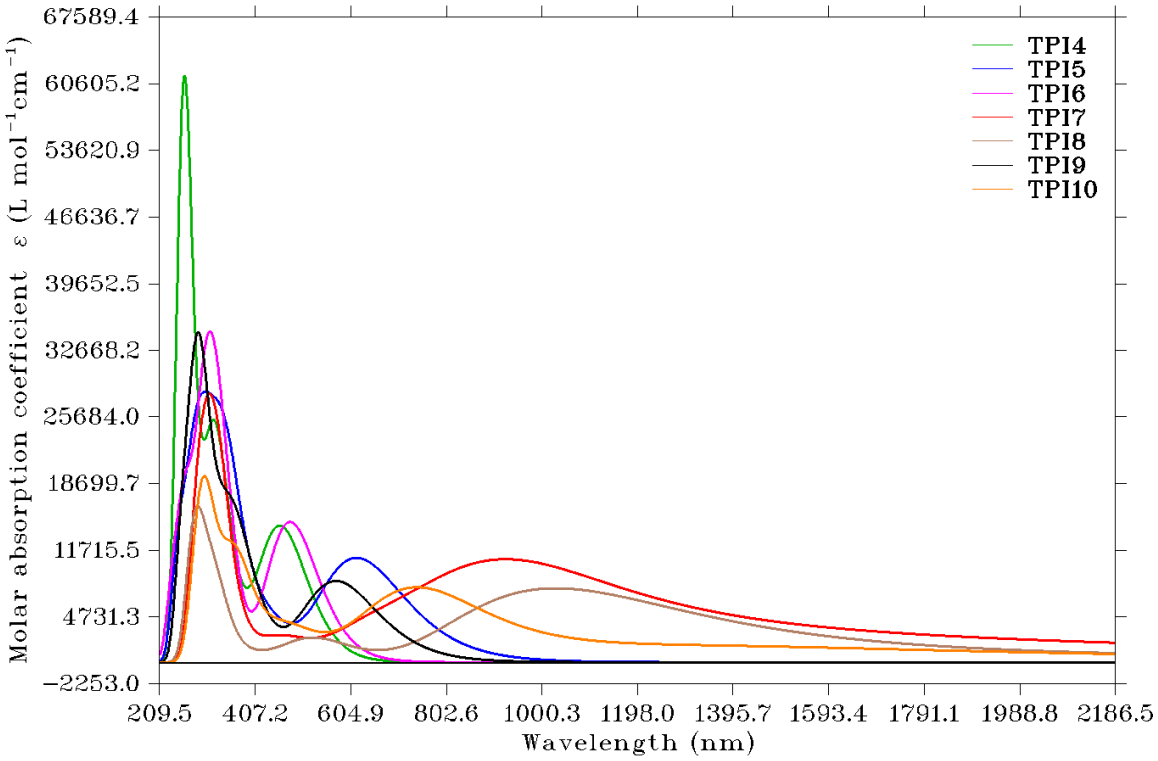

Figure 5: UV-Visible absorption spectra of solvated compounds possessing cyanoacetic acceptors (TPI4-TPI10) at 6-31+G(d,p) level.

CONCLUSION

Attachment of Donor and Acceptor groups through the imidazole' π-spacer was applied in this study to enhance the photo-electronic properties of 2,4,5-triphenyl imidazole. From our findings, the cyanoacetic accceptor units is observed to play a very significant role in improving the photo-electronic properties of 2,4,5-triphenyl imidazole. From the results from this study, ΔG_{inject} was observed to have the largest injection in TPI6 (-0.86 eV) than other compound observed in this study. The absorbance data describes how, only dyes with cyanoacetic acceptor units tend to absorb both visible and Uv light which is a prerequisite a DSSC dye must satisfy. These findings are however, a useful lead towards future experimental DSSC designs.

REFERENCES

1. F. Santoro, A. Lami, R. Improta, J. Bloino, and V. Barone (2008). Effective method for the computation of optical spectra of large molecules at finite temperature including the Duschinsky and Herzberg–Teller effect: The Q x band of porphyrin as a case study. *Journal of Chemical*

ISSN 0795 - 22066

Physics, 128 (22), 224311. https://doi.org/10.1063/1.2929846

2. J. M. Juma, S. A. H. Vuai, N. Surendra Babu, and N. S. Babu (2019). TD-DFT investigations on optoelectronic properties of fluorescein dye derivatives in dye-sensitized solar cells (DSSCs). *International Journal of Photoenergy*, 2019, 1–9 https://doi.org/10.1155/2019/4616198

3. F. Agda, T. Abram, M. Taleb, H. Taoufik, L. Bejjit, and M. Bouachrine (2015). Organic materials based on oxathiazole and thiophene for photovoltaic devices. Correlation structure/electronic properties. *Journal of Materials and Environmental Sciences*. 6 (6), 1733–1739.

4. A. El Assyry, R. Jdaa, B. Benali, M. Addou, and A. Zarrouk. (2015). Optical and photovoltaic properties of new quinoxalin-2 (1H)-one-based DA organic dyes for efficient dye-sensitized solar cell using DFT," *Journal of Materials and Environmental Sciences*. 6 (9), 2612–2623

5. P. Lianos (2017). Review of recent trends in photoelectrocatalytic conversion of solar energy to electricity and hydrogen. *Applied Catalysis B: Environmental*. 210, 235–254.

6. G. W. Crabtree and N. S. Lewis. (2007). Solar energy conversion. *Physics Today*. 60 (3) 37–42.

7. G. C. dos Santos, E. F. Oliveira, F. C. Lavarda, and L. C. da Silva-Filho. (2019). Designing new quinoline-based organic photosensitizers for dye-sensitized solar cells (DSSC): a theoretical investigation. *Journal of Molecular Modelling*. 25 (3). https://doi.org/10.1007/s00894-019-3958-y

8. D. Casanova (2011). The Role of the π Linker in Donor–π–Acceptor Organic Dyes for High-Performance Sensitized Solar Cells. *ChemPhysChem*, 12 (16), 2979–2988.

9. A. Fitri, A. T. Benjelloun, M. Benzakour, M. McHarfi, M. Hamidi, and M. Bouachrine. (2014). Theoretical investigation of new thiazolothiazole-based D-π-A organic dyes for efficient dye-sensitized solar cell. *Spectrochimica Acta Part A: Molecular and Biomolecular Spectroscopy*. 124 (1), 646–654 https://doi.org/10.1016/j.saa.2014.01.052

10. S. Das Sharma, P. Hazarika, and D. Konwar. (2008). An efficient and one-pot synthesis of 2, 4, 5-trisubstituted and 1, 2, 4, 5-tetrasubstituted imidazoles catalyzed by InCl3· 3H2O. *Tetrahedron Letter*. 49 (14), 2216–2220.

11. T. Prisinzano . H. Law, M. Dukat, A. Slassi, N. MaClean, L. Demchyshyn and R. A. Glennon. (2001). Imidazoline-modified benzylimidazolines as H5-HT1D/1B serotonergic ligands. *Bioorganic Medicinal Chemistry*. 9 (3), 613–619.

ISSN 0795 - 22066

12. S. Bhor, G. Anilkumar, M. K. Tse, M. Klawonn, C. Döbler, B. Bitterlich, A. Grotevendt and M. Beller. (2005). Synthesis of a new chiral N, N, N-tridentate pyridinebisimidazoline ligand library and its application in Ru-catalyzed asymmetric epoxidation. *Organometallic Letter.* 7 (16), 3393–3396.

13. J. G. Lombardino and E. H. Wiseman. (1974). Preparation and anti-inflammatory activity of some nonacidic trisubstituted imidazoles. *Journal of Medicinal Chemistry.* 17 (11), 1182–1188.

14. X. Chen, C. Jia, Z. Wan and X. Yao. (2014). Organic dyes with imidazole derivatives as auxiliary donors for dye-sensitized solar cells: Experimental and theoretical investigation, *Dyes and Pigments*, 104, 48-56.

15. I. N. Obotowo, I. B. Obot, and U. J. Ekpe. (2016). Organic sensitizers for dye-sensitized solar cell (DSSC): Properties from computation, progress and future perspectives. *Journal of Molecular Structure*, 1122, 80–87. https://doi.org/10.1016/j.molstruc.2016.05.080

16. M. Bourass, A. Touimi Benjelloun, M. Benzakour, M. Mcharfi, M. Hamidi, S.M. Bouzzine, F. Sereine-Spirau, T. Jarrosson, J. P. Lère-Porte, J. M. Sotiropoulos, M. Bouachrine. (2016). The computational study of the electronic and optoelectronics properties of new materials based on thienopyrazine for application in dye solar cells," *Journal of Materials and Environmental Sciences.* 7 (3), 700–712.

17. M. J. Frisch, G.W.T., H. B. Schlegel, G. E. Scuseria, M. A. Robb, J. R. Cheeseman, G. Scalmani, V. Barone, G. A. Petersson, H. Nakatsuji, X. Li, M. Caricato, A. Marenich, J. Bloino, B. G. Janesko, R. Gomperts, B. Mennucci, H. P. Hratchian, J. V. Ortiz, A. F. Izmaylov, J. L. Sonnenberg, D. Williams-Young, F. Ding, F. Lipparini, F. Egidi, J. Goings, B. Peng, A. Petrone, T. Henderson, D. Ranasinghe, V. G. Zakrzewski, J. Gao, N. Rega, G. Zheng, W. Liang, M. Hada, M. Ehara, K. Toyota, R. Fukuda, J. Hasegawa, M. Ishida, T. Nakajima, Y. Honda, O. Kitao, H. Nakai, T. Vreven, K. Throssell, J. A. Montgomery, Jr., J. E. Peralta, F. Ogliaro, M. Bearpark, J. J. Heyd, E. Brothers, K. N. Kudin, V. N. Staroverov, T. Keith, R. Kobayashi, J. Normand, K. Raghavachari, A. Rendell, J. C. Burant, S. S. Iyengar, J. Tomasi, M. Cossi, J. M. Millam, M. Klene, C. Adamo, R. Cammi, J. W. Ochterski, R. L. Martin, K. Morokuma, O. Farkas, J. B. Foresman, and D. J. Fox, Gaussian 09, Revision C.01. Gaussian, Inc., Wallingford CT., 2010

18. M. D. Hanwell, D. E. Curtis, D. C. Lonie, T. Vandermeersch, E. Zurek, and G. R. Hutchison. (2012). Avogadro: an advanced semantic chemical editor, visualization, and analysis platform," *Journal of Cheminformatics.* 4 (1), 1–17.

ISSN 0795 - 22066

19. T. Lu and F. Chen. (2012). Multiwfn: a multifunctional wavefunction analyzer. *Journal of Computational Chemistry.* 33 (5), 580–592.

20. T. J. Smith and K. J. Stevenson. (2021). Origin 7.5. OriginLab Corporation, One Roundhouse Plaza, Northampton, MA 01060. 1-800-969-7720. www.OriginLab.com

21. N. Mills. (2006). ChemDraw Ultra 10.0 CambridgeSoft, 100 Cambridge-Park Drive, Cambridge, MA 02140. www.cambridgesoft.com.

22. A. D. Becke. (1988). Density-functional exchange-energy approximation with correct asymptotic behavior, *Physical Review: A.* 38 (6), 3098.

23. I. S. John Wiley & Sons. (2022). Spectra Base Compound ID=9SRNf0LZw3y Spectra Base Spectrum ID=CQvQtF3tfGk.. https://spectrabase.com/spectrum/CQvQtF3tfGk

24. J. K. Roy, S. Kar, and J. Leszczynski (2019). Electronic Structure and Optical Properties of Designed Photo-Efficient Indoline-Based Dye-Sensitizers with D–A– π –A Framework. *Journal of Physical Chemistry C.* 123 (6), 309–3320 https://doi.org/10.1021/acs.jpcc.8b10708

25. J. Zhang, H. B. Li, S.-L. Sun, Y. Geng, Y. Wu, and Z. M. Su. (2012). Density functional theory characterization and design of high-performance diarylamine-fluorene dyes with different π spacers for dye-sensitized solar cells. *Journal of Material Chemistry. 22 (2),* 568–576.

26. G. Pourtois, D. Beljonne, J. Cornil, M. A. Ratner, and J. L. Brédas. (2002). Photoinduced electron-transfer processes along molecular wires based on phenylenevinylene oligomers: a quantum-chemical insight. *Journal of American Chemical Society.* 124 (16), 4436–4447.

27. C.-P. Hsu. (2009). The electronic couplings in electron transfer and excitation energy transfer. *Account of Chemical Research.* 42 (4), 509–518.

28. R. A. Marcus. (1993). Electron transfer reactions in Chemistry: Theory and experiment (Nobel lecture). *Angewandte Chemie International Edition* (English), 32 (8), 1111–1121.

29. O. B. Malcıoğlu, A. Calzolari, R. Gebauer, D. Varsano and S. Baroni. (2011). Dielectric and thermal effects on the optical properties of natural dyes: A case study on solvated cyanin. *Journal of American Chemical Society.* 133 (39), 15425–15433, https://doi.org/10.1021/ja201733v

ISSN 0795 - 22066